Proceedings of the 7th International Conference on Mechanics and Materials in Design
Albufeira/Portugal 11-15 June 2017. Editors J.F. Silva Gomes and S.A. Meguid.
Publ. INEGI/FEUP (2017)

PAPER REF: 6442

ASSESSMENT OF A SUBSTITUTE BIRD MODEL FOR THE PREDICTION OF BIRD-STRIKE OF HELICOPTERS STRUCTURES

David Delsart[1(*)], Florent Boyer[3], Alice Vagnot[2]
[1]ONERA Centre de Lille, DADS/CRD, Lille, France
[2]AIRBUS Helicopters, ETVSR, Marignane, France
[3]AIRBUS Helicopters, ETVSR, Donauwörth, Germany
[(*)]*Email:* david.delsart@onera.fr

ABSTRACT

The paper addresses a collaborative project involving AIRBUS Helicopters and ONERA (Office National d'Etudes et de Recherches Aérospatiales), whose objective targeted the improvement of helicopters structures resistance to bird-strikes. In that frame, technical activities aimed at identifying a bird substitute material specific to the helicopter flight domain, to replace real birds, first, in development tests and, finally, in certification tests, and at developing its modeling methodology through correlations with instrumented impact tests.

Keywords: modelling, substitute, bird, helicopter.

INTRODUCTION

Bird strike incidents could constitute, in certain circumstances, a significant threat for rotorcraft safety. Manufacturers of heavy helicopters have to prove the compliance of their vehicles with existing standards (CS-29 / FAR Part 29), which require that they "must be designed to assure capability of continued safe flight and landing (for Category A) or safe landing (for Category B) after impact with a 1kg bird, when the velocity of the rotorcraft (relative to the bird along the flight path of the rotorcraft) is equal to VNE (Never exceed speed) or VH (Maximum speed in level flight at maximum continuous power), whichever is the lesser, at altitudes up to 2438m (8000ft). Compliance must be shown by tests or by analysis based on tests carried out on sufficiently representative structures of similar design". Numerical analysis is today broadly widespread in the aircraft industry insofar it represents a cost-effective technique for the development of innovative products, for it allows to confront, in the earlier stage of the development process, a wide range of designs to certification requirements, while minimizing the reliance to expensive full-scale tests.

In that field, AIRBUS Helicopters set up a research programme that aimed at improving the resistance of helicopters to bird-strikes, which covered, on the experimental side, the definition of a bird substitute material specific to the helicopter flight domain (90m/s typical flight velocity), to be used as a replacement projectile to the possibly dispersive real birds, and, on the numerical side, the assessment of modelling techniques for bird-strike (with the explicit code RADIOSS - ALTAIR company), starting with the validation of a bird substitute material model. In a preliminary step, AIRBUS Helicopters, in cooperation with the DGA Ta test centre (Direction Générale de l'Armement - Techniques aéronautiques), thus identified a bird substitute (gelatine material) whose performances and representativeness compared to real birds were validated through a preliminary programme of impact tests on rigid targets; it involved, on the one hand, flat plates instrumented with pressure transducers distributed over

the impact area, thus enabling to correlate the pressure response profile between the gelatine material and the real birds, and, on the other hand, cutting edges to analyse the splitting of the projectile. This material was applied in the following of the project.

IMPACT TESTS PROGRAMME

In the perspective of validation of the bird substitute material model, an impact tests program was performed including 2 complementary sets of tests - to take into account the potential difference in the projectile kinematics according to the target deformability - with, on the one hand, impacts on a rigid target and, on the other hand, impacts on thin aluminium plates. In both cases, the gelatine projectiles presented the dimensions described in the figure on the right, leading to a 1Kg mass.

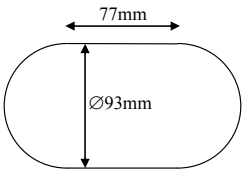

Fig. 1 - Dimensions of the gelatin projectiles for the impact tests program

The whole test program was performed at the DGA Ta test facility which utilizes a Ø=150mm and L=9m gas gun.

Impact tests on a rigid target

The rigid target is made of a 30mm thick circular rigid plate supported by 3 piezoelectric load cells. This assembly is inserted inside a massive aluminium rig whose external surface is flush with the circular plate, so that not to perturb the spreading of the projectile. The whole set-up is finally maintained vertical by the mean of 2 metallic brackets fixed to the ground.

Measurements comprise the evolution of the impact force resulting from the summation of the 3 load cell signals and videos from 2 high speed cameras (side and ¾ views) operating at a 10000 frames/s rate.Two sets of tests are performed, at the average velocities of 47m/s and 90m/s. Their results are presented in the following figures, in terms of force versus time. One can observe the presence of oscillations resulting from the resonance of the rig system, at an average frequency of 2,7KHz.


Fig. 2 - Configuration of the impact tests on a rigid target (DGA Ta)

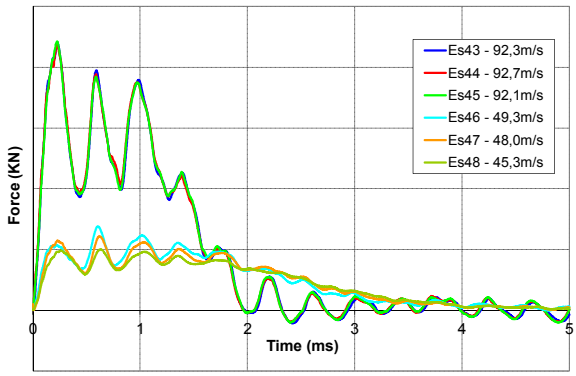

Fig. 3 - Results of the impact tests at 47m/s and 90m/s

Impact tests on aluminum plates

The configuration of the impact tests on deformable targets is shown in Fig.. The rig is made of a rectangular frame attached, by the means of 3 load sensors, to an orientable rigid frame fixed to the ground. The targets are made of 920x620mm 2024-T3 aluminum plates which are bolted at their periphery to the rectangular frame, with bolts regularly spaced by 60mm. Depending on the test velocity and rig orientation, their thickness varies from 0,8mm, 1,0mm to 1,4mm.

Measurements include:

- The residual deflection of the plate measured by three-dimensional mapping along 2 vertical and horizontal lines passing at the point of maximal deflection.
- The impact force as the summation of the force signals from the 3 load sensors connecting the rectangular frame to the orientable rigid frame.
- DIC (Digital Image Correlation) measures by the means of 2 high speed cameras positioned behind the aluminium plate. The post-treatment of the videos notably enables to identify the evolution of the plate deflection during the impact (at the impact point).

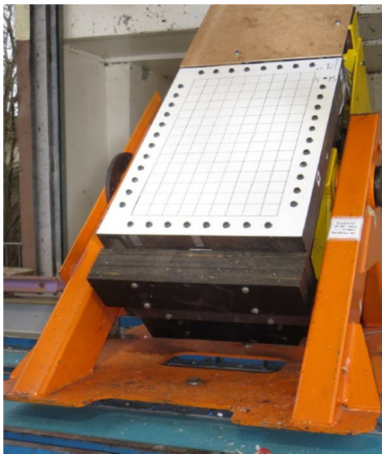

Fig. 4 - Test rig for the impact tests on deformable targets (DGA Ta)

- Videos from a high speed camera operating at a 10000 frames/s rate, in frontal 3/4 view.

The test plan covers different impact velocities, from 47m/s to 115m/s, and 2 orientations, 90° and 45°. Let's note that in a prior step, impact tests with a rigid metallic ball (Ø=25mm) at 90m/s & 90° were also conducted so as to validate the FE model of the aluminum plate, considered as a sensor.

Among all tested configurations, the case 47m/s & 45° which results in the lowest impact energy, as a combination of the low velocity and the orientation, is characterized by a specific behavior of the projectile that one may no more qualify of hydrodynamic type, where the projectile dos not spread but keeps a relative consistence.

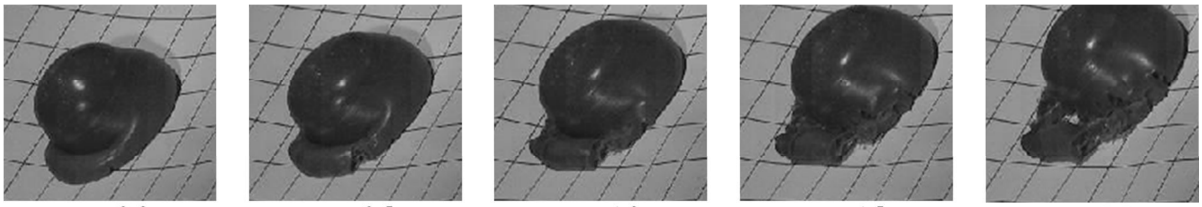

Fig. 5 - Visualization of the projectile deformation for the impact at 47m/s & 45°

MODELLING

Gelatin projectile model

Many works performed in the past decades to analyse the behaviour of birds subject to high-velocity impacts have demonstrated that such impacts could be assumed of hydrodynamic type, with the bird exhibiting a fluid-like behaviour (Wilbeck, 1981). Diverse equations of state have been proposed (Barber, 1975) and different formulations have been evaluated (Brockman, 1991 / Langrand, 2002 / Lavoie, 2007 / Heimbs, 2011 / Ugrcic, 2012), from standard Lagrangian formulations to more recent methods for soft body modelling, such as Arbitrary Lagrangian Eulerian (ALE) and Smooth Particle Hydrodynamics (SPH). Within the project, the SPH formulation was selected and a hydrodynamic model described by a polynomial equation of state defining the evolution of the pressure with the volume variation (1) was applied.

$$P = C_0 + C_1\mu + C_2\mu^2 + C_3\mu^3 + (C_4 + C_5\mu)E_0 \quad \text{with} \quad \mu = \frac{\rho}{\rho_0} - 1 = -\frac{\Delta V}{V} \tag{1}$$

The inter-particles distance was set to h_0=6mm, leading to a 6100 particles projectile model, and the material parameters, mainly reducible to the C_1 parameter representative of the compressibility module K, were calibrated so as to best correlate with the impact tests on the rigid target.

Simulation of the impact tests on rigid target

Insofar tests exhibited oscillations due to the resonance of the rig system and considering that no specific boundary within the rig was clearly distinguishable, apart from the brackets fixing to the ground, one decided to fully model the rig system, as shown in Fig., using mostly 3D elements associated to elastic laws and standard material parameters. The load cells are modelled similarly, attributing initial material parameters coming from the manufacturer's data. Load sections are generated across each load cell, thus enabling to calculate, by summation over the 3 cells, the impact force for comparison with the experiments.

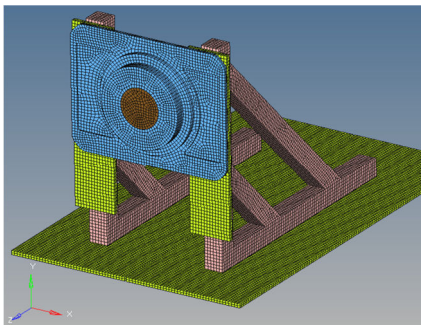

Fig. 6 - Model of the test rig for the impacts on rigid target

The accent was brought to the selection of the appropriate elements formulations, the adaptation of the load cell material parameters, and the connection of the load cells to their environment, to conveniently capture the experimentally observed frequency.

Simulations are performed in a single run, over a 3ms duration for the impacts at 90m/s, and 5ms for those at 47m/s. Results are presented in the following figure for the 2 velocities, in terms of force/time evolution and visualizations at increasing times in frontal ¾ view, compared to the experimental measurements.

- For the 90m/s impacts, though the frequency of the rig remains slightly underestimated (~2,4 Hz), a convenient level of correlation is however reached, with a reasonable prediction of the successive load pics until the final signal attenuation. Besides, the visualizations of the impact at increasing times show a spreading of the projectile comparable with the experimental observations.

- For the 47m/s impacts, the correlation globally remains satisfactory, even though the initial load pic is slightly overestimated by the model. The spreading of the projectile also fits conveniently with the experiment.

Simulation of the impact tests on deformable targets

For simplification reasons, the modelling of the rig system of the impact tests on deformable targets is limited to the aluminum plate, the supporting rectangular frame and the 3 load sensors with their junction components - i.e. the orientable frame is not modelled. Consequently, fixed boundary conditions are applied on the flanges of these junction components. Such a simplification may not show any influence in terms of deflection (dynamic or residual) but may in terms of impact force as the orientable frame, by its own flexibility, would tend to attenuate/damp the load sensor responses. To bypass this issue, one

therefore applies a damping coefficient on the whole model, aluminum plate excluded, a 0,8 value being shown appropriate to best correlate the force measurements.

The aluminum plate is modeled with shell elements with a mesh size of 5mm at the center of the plate plaque, and degressive towards its periphery. Elements are associated to an elasto-plastic Johnson-Cook model with standard parameters coming from previous projects. The load sensors are modelled with uniaxial spring elements with their stiffnesses calculated from their dimensions and constitutive material.

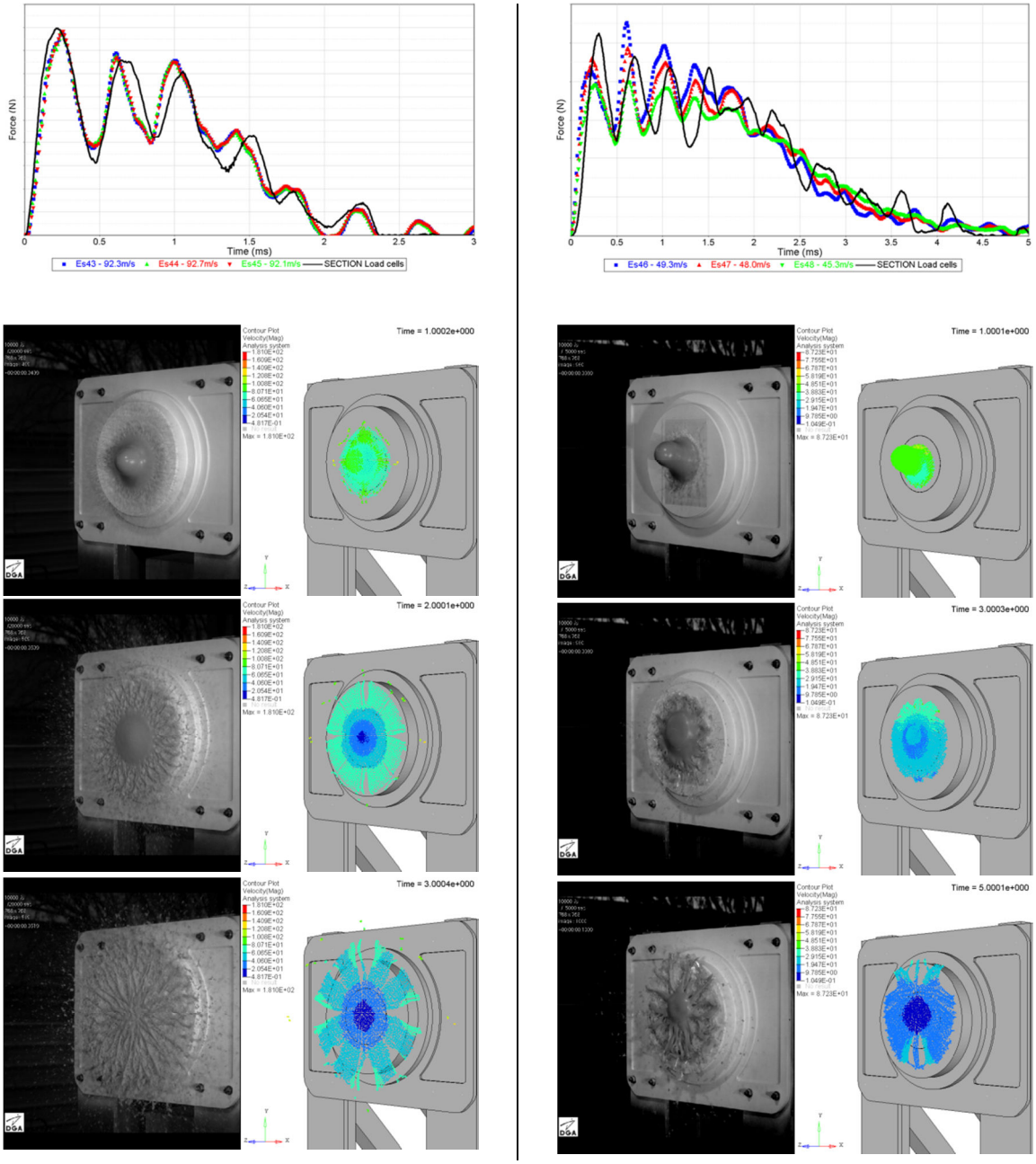

Fig.7 - Numerical/experimental comparison: (a) Impact at 90m/s, (b) Impact at 47m/s

Finally, a specific emphasis was brought to the modelling of the bolts attaching the aluminum plate to the rectangular frame. As indeed illustrated in Fig. 8 for one test at 90m/s & 90°, tests highlighted noticeable deformation of the aluminum plate around the bolted areas, resulting in an obvious contribution on the global plate behavior. A fine modelling of these local phenomenon being excluded within the project, one opted to model the plate deformation through the shear elongation of the multi-axial springs representing the bolts i.e. the springs behavior in their shear direction are calibrated to allow tangential displacement of the points of connection between the plate and the frame.

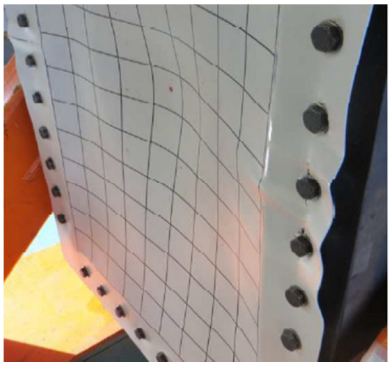

Fig. 1 - Illustration of the plate deformations at the bolted areas

The identification of the shear responses requiring at least 2 points, this calibration is therefore performed on 2 configurations, including first the impacts at 90m/s with the Ø=25mm ball, and then the impacts at 90m/s & 90° with the gelatin projectile; once achieved, this was applied on the other configurations. Most of simulations confirmed the role and amplitude of these deformations in the measured signals, firstly in terms of the plate dynamic or residual deformation, but also in terms of force signal, as discussed in the following paragraphs.

Simulations are conducted in 2 successive runs, the first one over 20ms corresponding to the simulation of the impact, and the second one over an additional 40ms to allow the elastic return of the plate up to its final state (activation of a kinematic relaxation option), so as to permit the comparisons with the residual deflection measurements. The following paragraphs illustrate typical results obtained within the simulated impact configurations, including the impacts at 90m/s & 90°, 90m/s & 45°, 115m/s & 90°, 60m/s & 90° and 47m/s & 45°.

In the following pages, numerical results are confronted to the experimental data in terms of dynamic deflection of the plate (i.e. during run 1), residual deflection of the plate (i.e. after run 2) along the length (section 1) and the width (section 2) of the plate, and impact force coming from the load sensors (i.e. during run 1). Moreover, a qualitative comparison is also provided with the visualization of the projectile spreading over the first 5ms of the impact.

Apart for the configuration at 45m/s & 45° which exhibited a specific projectile behaviour and that will be analysed separately, all configurations led to comparable conclusions that are summarized hereafter:

- One first notes that, to obtain a convenient correlation, notably in terms of dynamic deflection, the calibration of the spring elements representing the bolts, performed on the impact at 90m/s & 90°, leads to a shear elongation of 2,7mm in the most loaded spring. When applied to the rest of the configurations (see following table), this maximal elongation extends from 1,9mm for the lowest impact energy (60m/s & 90) to 3,3mm for the highest one (115m/s & 90°), which confirms the significant influence of the bolted areas in the plate behavior.

Table 1 - Shear elongation in the most loaded spring

Impact configuration	**90m/s & 90°**	**90m/s & 45°**	**115m/s & 90°**	**60m/s & 90°**
Elongation (mm)	2,7	2,2	3,3	1,9

- Whatever the observable, the correlation is globally satisfying with deviations between numerical and experimental maximal data that never exceed 11%, as shown in the following tables.

Table 2 - Numerical/experimental comparison for the impact at 90m/s & 90°

Data	Max dynamic deflection	Max residual deflection	Maximal force
Deviation simulation/test	*-4%*	*+8%*	*+4%*

Table 3 - Numerical/experimental comparison for the impact at 90m/s & 45°

Data	Max dynamic deflection	Max residual deflection	Maximal force
Deviation simulation/test	*+3%*	*0%*	*+2%*

Table 4 - Numerical/experimental comparison for the impact at 115m/s & 90°

Data	Max dynamic deflection	Max residual deflection	Maximal force
Deviation simulation/test	*/*	*+3%*	*+7%*

Table 5 - Numerical/experimental comparison for the impact at 60m/s & 90°

Data	Max dynamic deflection	Max residual deflection	Maximal force
Deviation simulation/test	*-11%*	*-2%*	*+10%*

- Besides, the visualization of the projectile spreading illustrated for each impact configuration shows, in average, a convenient behavior of the projectile, at least up to 5ms i.e. beyond the actual duration of the impact phase.

For the configuration at 47m/s & 45°, results are noticeably different; though it still correlates well in the first milliseconds of the impact (as shown by the correct prediction of the maximum dynamic deflection and of the force signal in the initial phase of the impact), the calculation then largely diverges from the experiment, be it quantitatively with a large underestimation of the residual deflection and of the second force pic, or qualitatively with an inappropriate modelling of the projectile, that still spreads in the simulation while remains quite compact during the test.

Table 6 - Numerical/experimental comparison for the impact at 47m/s & 45°

Data	Max dynamic deflection	Max residual deflection	Maximal force
Deviation simulation/test	*+7%*	*-32%*	*-39%*

Insofar the projectile here rather behaves like a solid medium than a hydrodynamic one, one may wonder if these issues are symptomatic of the limits of application of the SPH formulation and/or of the material model. To answer this question, a simulation is therefore performed using 3D elements for the projectile and shows similar results, leading to the conclusion that the material model and its parameters are not adapted to low energy impacts where the projectile no more fully breaks up. Though improvements may be reachable by playing on some of the material parameters, but at the expense of the other configurations, no further effort was engaged to better correlate this configuration that is either way not critical in terms of dimensioning.

Impact at 90m/s & 90°

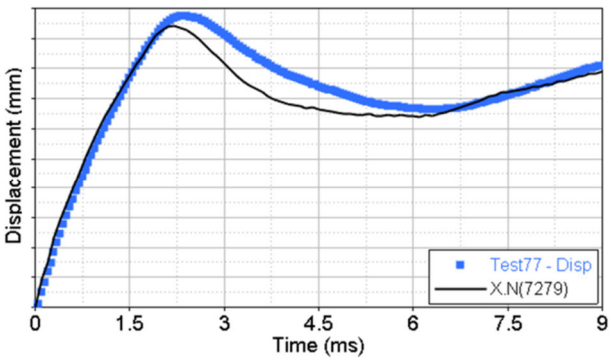

Fig. 9 - Dynamic deflection

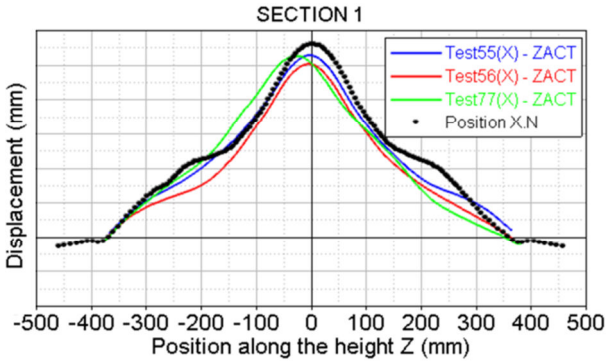

Fig. 10 - Residual deflection along section 1

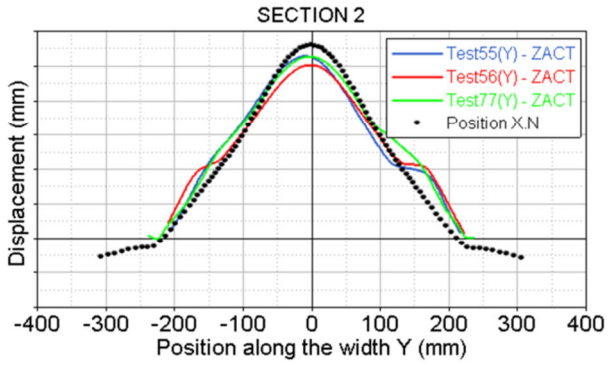

Fig. 11 - Residual deflection along section 2

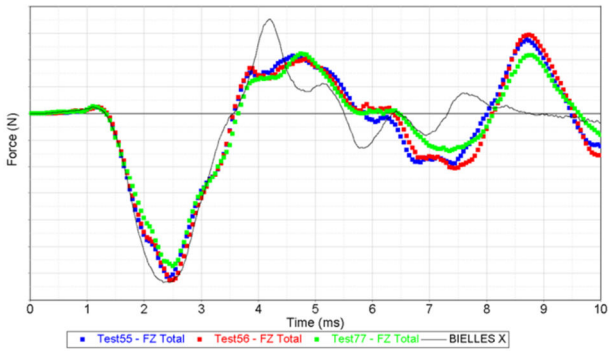

Fig. 12 - Impact force

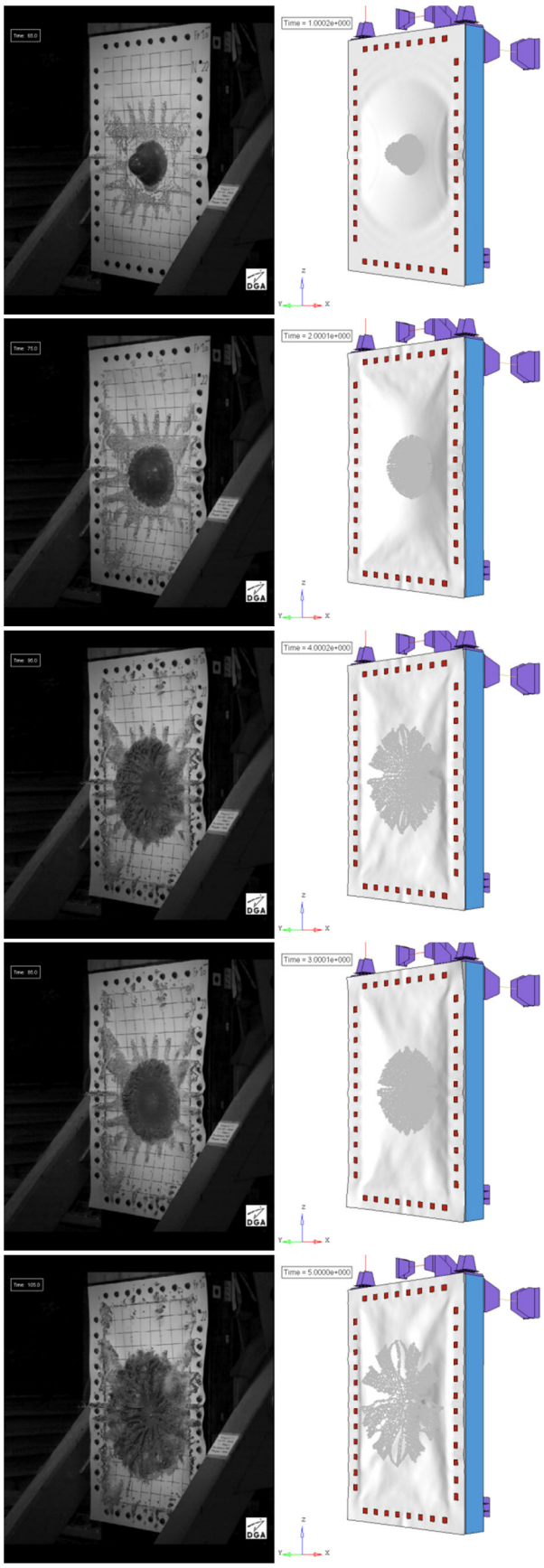

Fig. 13 - Impact sequence from 1ms to 5ms

Impact at 90m/s & 45°

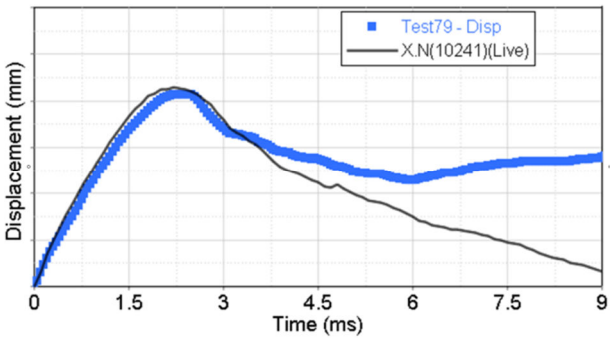

Fig. 14 - Dynamic deflection

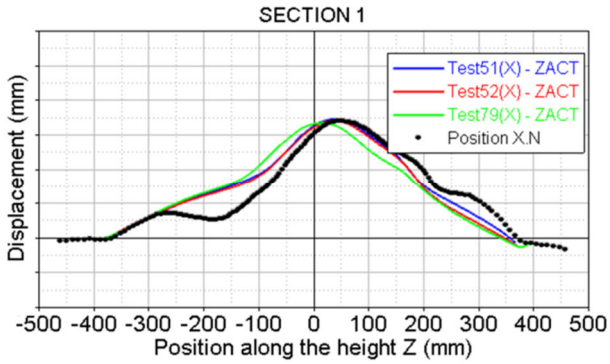

Fig. 15 - Residual deflection along section 1

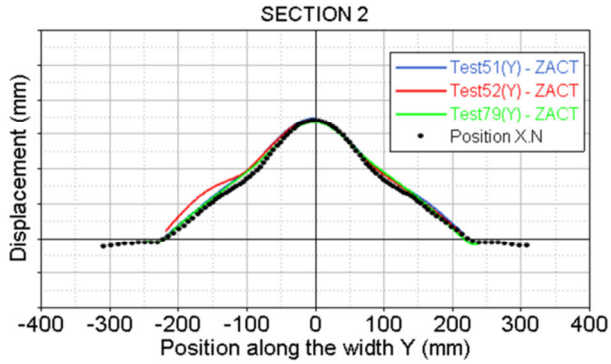

Fig. 16 - Residual deflection along section 2

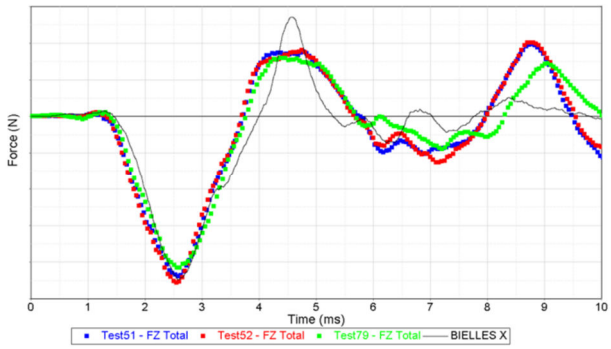

Fig. 17 - Impact force

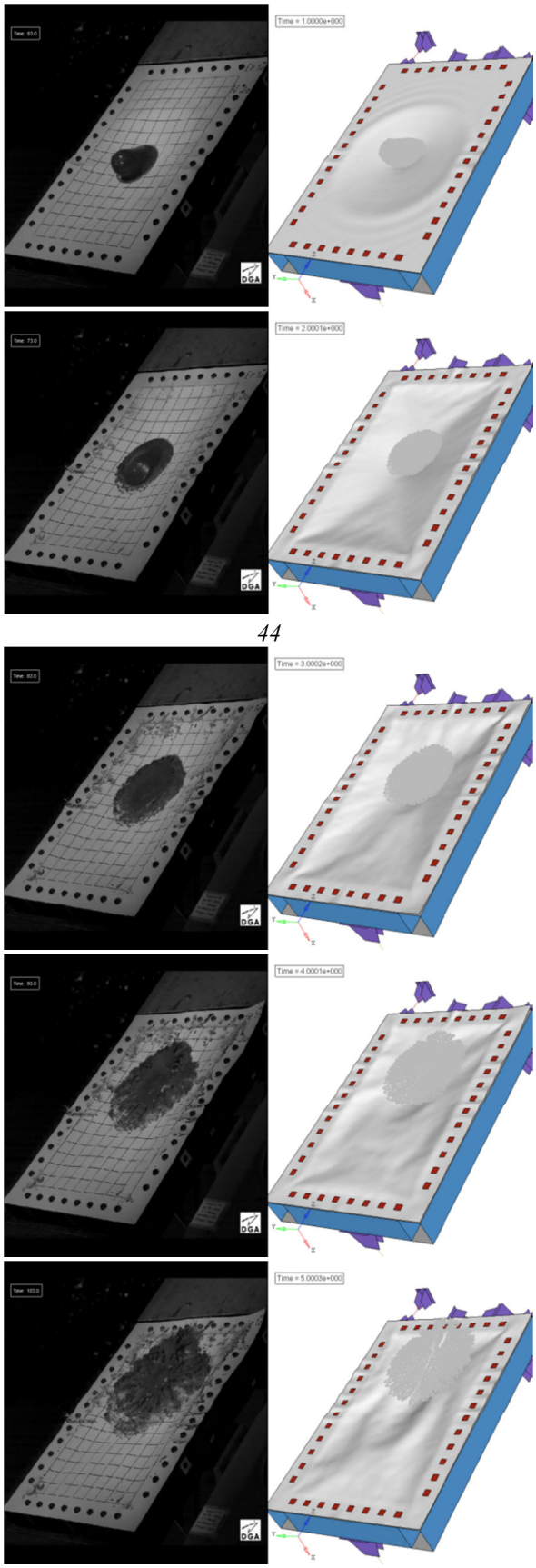

Fig. 18 - Impact sequence from 1ms to 5ms

Impact at 115m/s & 90°

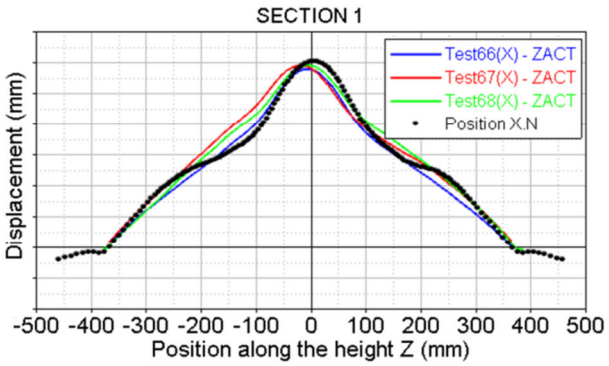

Fig. 19 - Residual deflection along section 1

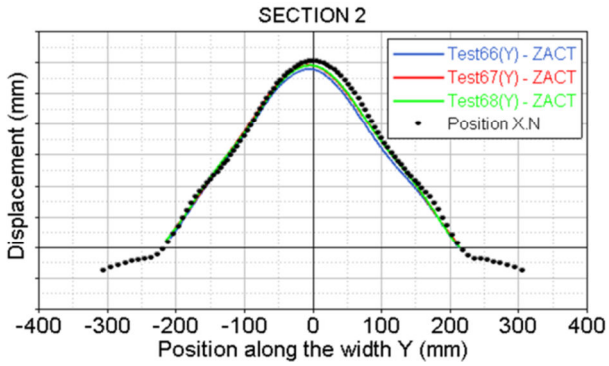

Fig. 20 - Residual deflection along section 2

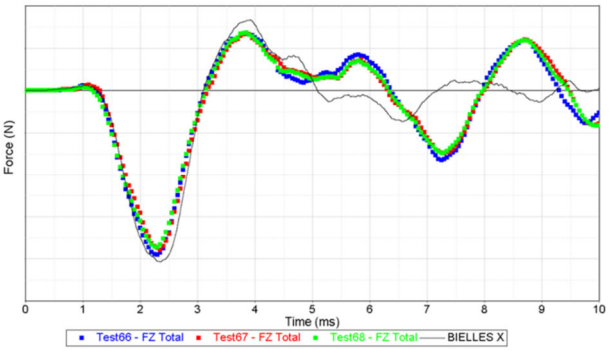

Fig. 21 - Impact force

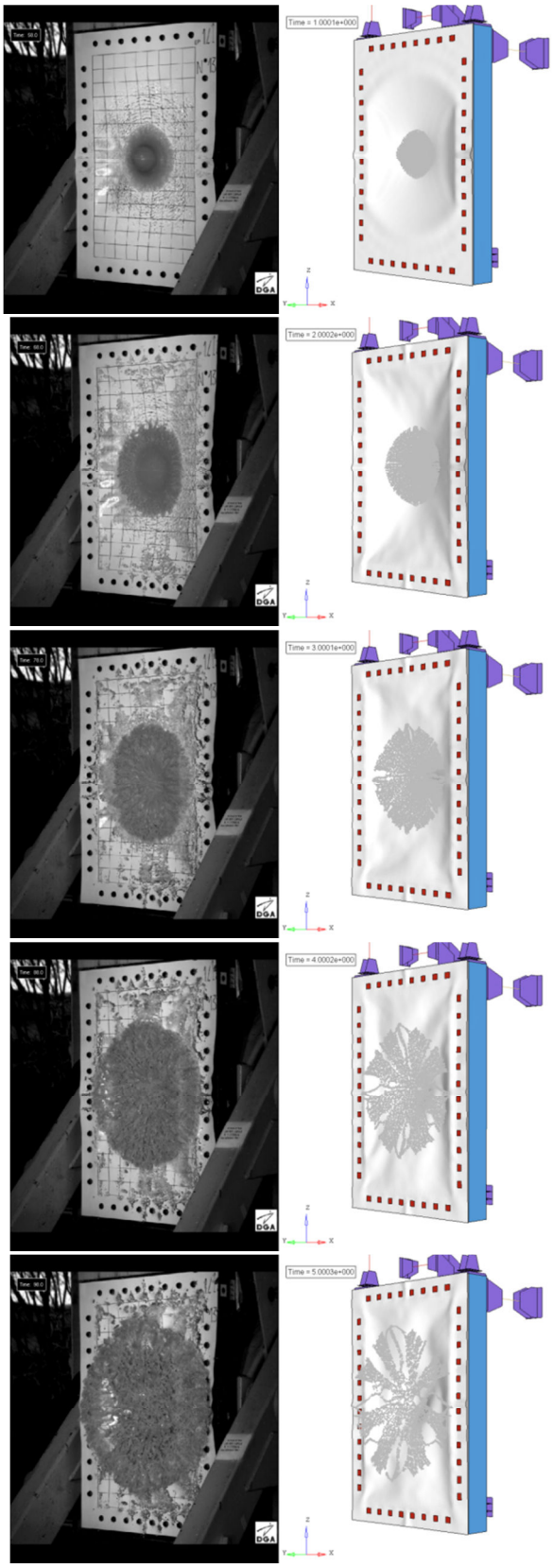

Fig. 22 - Impact sequence from 1ms to 5ms

Impact at 60m/s & 90°

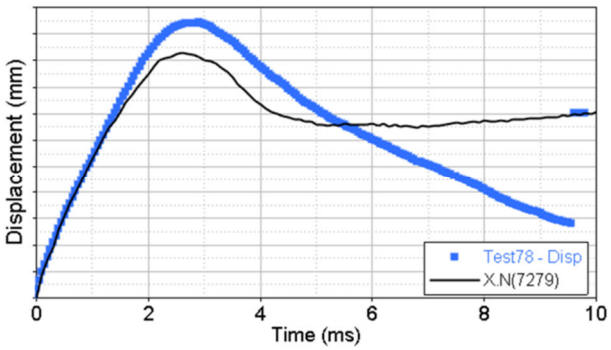

Fig. 23 - Dynamic deflection

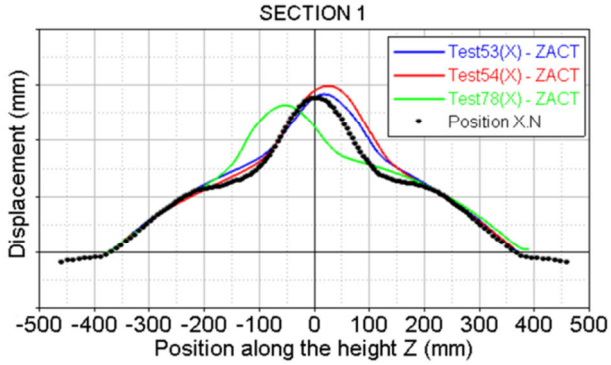

Fig. 24 - Residual deflection along section 1

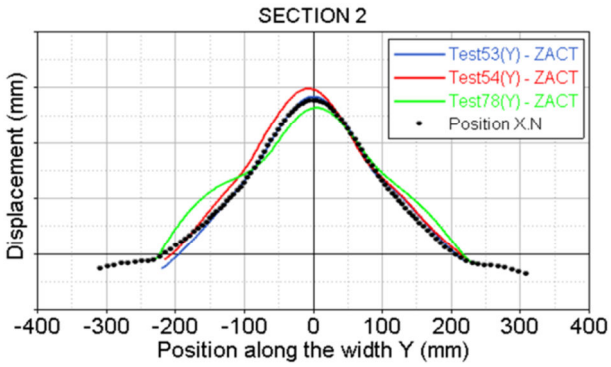

Fig. 25 - Residual deflection along section 2

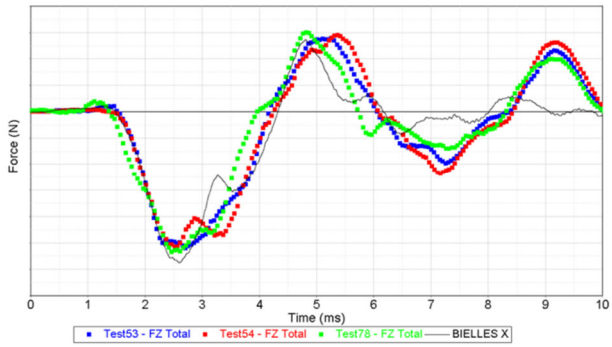

Fig. 26 - Impact force

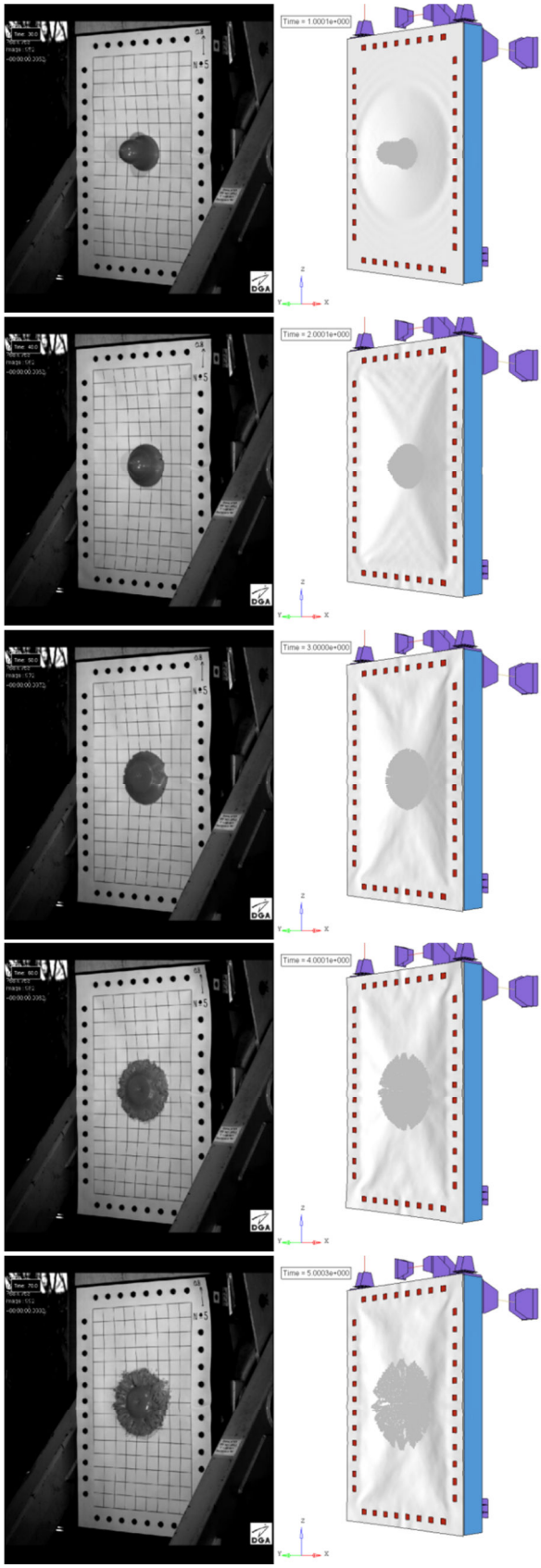

Fig. 27 - Impact sequence from 1ms to 5ms

Impact at 47m/s & 45°

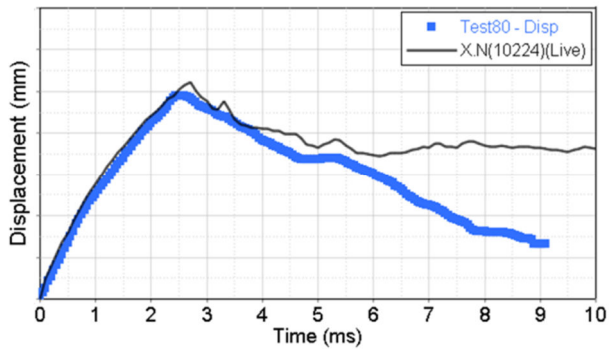

Fig. 2 - Dynamic deflection

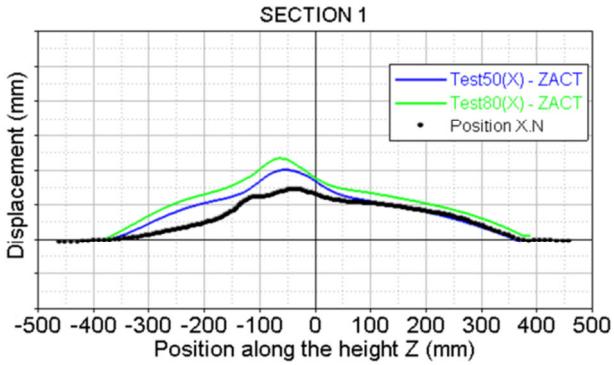

Fig. 3 - Residual deflection along section 1

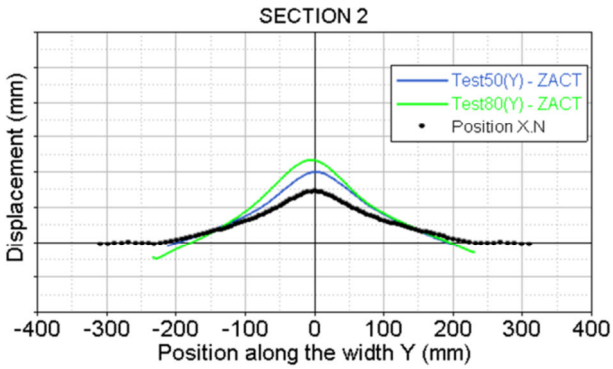

Fig. 4 - Residual deflection along section 2

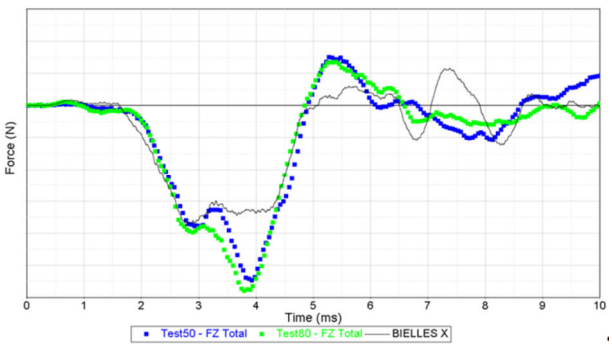

Fig. 5 - Impact force

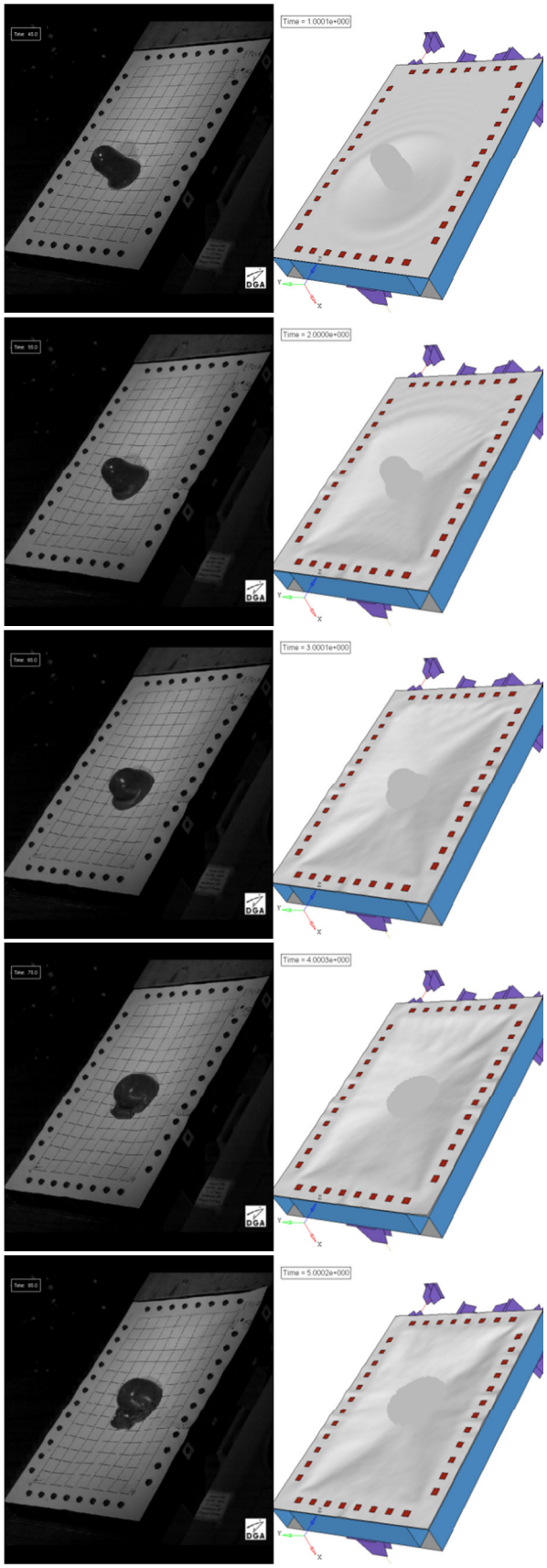

Fig. 6 - Impact sequence from 1ms to 5ms

CONCLUSIONS

The project, performed in cooperation with AIRBUS Helicopters and ONERA, aimed at identifying a bird substitute material specific to the helicopter flight domain and at developing its modeling methodology with the explicit code RADIOSS. These works were performed with the support of experimental data generated through an impact test program involving rigid and deformable targets, for a large range of impact configurations.

The modelling approach is based on an hydrodynamic material model, classically applied for simulating soft bodies exhibiting fluid-like behaviours, coupled with a SPH formulation. Generally speaking, correlation levels with the various observables, be it on the rigid or deformable targets, proved to be satisfying, notably around the 90m/s velocity representative of the helicopter flight domain, and thus confirmed the suitability of such models for simulating high velocity impacts. Works also permitted to discern the limits of application of the proposed modelling method when applied for low energy impacts which reflect into a projectile behavior that is no more purely hydrodynamic.

ACKNOWLEDGMENTS

Authors wish to acknowledge the French Ministry of Defense, the FEDER and the Région Nord-Pas-de-Calais. Authors also wish to acknowledge DGA Ta for its contribution to the test programmes and its technical support throughout the project.

REFERENCES

[1]-Wilbeck JS, Rand JL. “The development of a substitute bird model”. Journal of Engineering for Power, October 1981, Vol.103, p. 725-730.

[2]-Wilbeck JS. “Impact behavior of Low Strength Projectiles,” University of Dayton Research Institute for the Airforce Flight.

[3]-Barber JP, Taylor HR, Wilbeck JS. “Characterization of Bird Impacts on a Rigid Plate: Part 1”, Technical report AFFDL-TR-75-5, Air Force Flight Dynamics Laboratory, Wright-Patterson Air Force Base, OH (1975).

[4]-Brockman RA, Held TW. “Explicit Finite element method for transparency impact analysis,” Technical report, University of Dayton Research Institute, Wright Patterson Air Force Base, 1991.

[5]-Langrand B, Bayart AS, Chauveau Y, Deletombe E. "Assessment of multi-physics FE methods for bird strike modelling- Application to a metallic riveted airframe“ Journal of Crashworthiness, January, 2002, Vol. 7, Issue 4, p. 415-428.

[6]-Lavoie MA, Gakwaya A, Nejad Ensan N, Zimcik DG. "Validation of Available Approaches for Numerical Bird Strike Modeling Tools", International Review of Mechanical Engineering, May 2007, Vol 1, n° 4, p. 380-389.

[7]-Lavoie MA, Gakwaya A, Nejad Ensan N, Zimcik DG. "Review of existing numerical methods and validation procedure available for bird strike modelling", International conference on Computational & Experimental Engineering and Sciences", 2007, Vol. 2, n° 4, p. 111-118.

[8]-Heimbs S. "Bird Strike Simulations on Composite Aircraft Structures" 2011 SIMULIA Customer Conference.

[9]-Heimbs S. "Computational methods for bird strike simulations: a review" Computers & Structures, Volume 89, Issues 23-24, December 2011, p. 2093-2112.

[10]-Ugrcic M. "Application of the Hydrodynamic theory and the Finite element Method in the analysis of Bird Strike in a Flat Barrier", Scientific Technical Review, 2012, Vol. 62, n° 3-4, p. 28-37.